

ORIGINAL ARTICLE

Role of tetrahydrobiopterin in pulmonary vascular remodelling associated with pulmonary fibrosis

Patricia Almudéver,¹ Javier Milara,^{2,3,4,5} Alfredo De Diego,⁶ Ana Serrano-Mollar,^{5,7} Antoni Xaubet,^{5,8} Francisco Perez-Vizcaino,^{5,9} Angel Cogolludo,^{5,9} Julio Cortijo^{1,2,4,5}

► Additional material is published online only. To view please visit the journal online (<http://dx.doi.org/10.1136/thoraxjnl-2013-203408>).

¹Department of Pharmacology, Faculty of Medicine, University of Valencia, Valencia, Spain

²Clinical Research Unit (UIC), University General Hospital Consortium, Valencia, Spain

³Department of Biotechnology, Universidad Politécnica de Valencia, Valencia, Spain

⁴Research Foundation of General Hospital of Valencia, Valencia, Spain

⁵CIBERES, Health Institute Carlos III, Valencia, Spain

⁶Servicio de Neumología, Hospital Universitario y Politécnico La Fe, Valencia, Spain

⁷Dept de Patología Experimental, Instituto de Investigaciones Biomédicas de Barcelona, Consejo Superior de Investigaciones Científicas, Barcelona, Spain

⁸Servicio de Neumología, Hospital Clínico, Instituto de Investigaciones Biomédicas Agustí Pi Suñer (IDIBAPS), Barcelona, Spain

⁹Department of Pharmacology, School of Medicine, Universidad Complutense de Madrid, Madrid, Spain

Correspondence to

Dr Javier Milara, Unidad de Investigación, Consorcio, Hospital General Universitario, Avenida tres cruces s/n, Valencia E-46014, Spain; xmilara@hotmail.com

PA and JM contributed equally.

Received 10 February 2013

Revised 24 April 2013

Accepted 16 May 2013

Published Online First

5 June 2013

To cite: Almudéver P, Milara J, De Diego A, et al. *Thorax* 2013;**68**:938–948.

ABSTRACT

Background Pulmonary hypertension in idiopathic pulmonary fibrosis (IPF) is indicative of a poor prognosis. Recent evidence suggests that tetrahydrobiopterin (BH4), the cofactor of nitric oxide synthase (NOS), is involved in pulmonary hypertension and that pulmonary artery endothelial-to-mesenchymal transition (EnMT) may contribute to pulmonary fibrosis. However, the role of BH4 in pulmonary remodelling secondary to pulmonary fibrosis is unknown. This study examined the BH4 system in plasma and pulmonary arteries from patients with IPF as well as the antiremodelling and antifibrotic effects of the BH4 precursor sepiapterin in rat bleomycin-induced pulmonary fibrosis and in vitro EnMT models.

Methods BH4 and nitrotyrosine were measured by high-performance liquid chromatography and ELISA, respectively. Expression of sepiapterin reductase (SPR), GTP cyclohydrolase 1 (GCH-1), endothelial NOS (eNOS) and inducible NOS (iNOS) were measured by quantitative PCR and immunohistochemistry.

Results BH4 plasma levels were downregulated in patients with IPF compared with controls while nitrites, nitrates and nitrotyrosine were upregulated. GCH-1 and eNOS were absent in pulmonary arteries of patients with IPF; however, iNOS expression increased while SPR expression was unchanged. In rats, oral sepiapterin (10 mg/kg twice daily) attenuated bleomycin-induced pulmonary fibrosis, mortality, vascular remodelling and pulmonary hypertension by increasing rat plasma BH4, decreasing plasma nitrotyrosine and increasing vascular eNOS and GCH-1 expression. Both transforming growth factor β 1 and endothelin-1 induced EnMT by decreasing BH4 and eNOS expression. In vitro administration of sepiapterin increased endothelial BH4 and inhibited EnMT in human pulmonary artery endothelial cells.

Conclusions Targeting the BH4 synthesis 'salvage pathway' with sepiapterin may be a new therapeutic strategy to attenuate pulmonary hypertension in IPF.

INTRODUCTION

Idiopathic pulmonary fibrosis (IPF) is the most common idiopathic interstitial pulmonary disease. It is a fatal disorder with a median survival of 2.5–5 years as no effective treatment exists. Pulmonary hypertension is recognised as a severe complication of IPF associated with poor survival.¹ Recent epidemiology studies have reported a prevalence of pulmonary hypertension in IPF of 32–84% depending on the stage of IPF progression.¹ The pathogenesis of pulmonary hypertension in IPF reflects a multifactorial and complex process involving a variety of pathways and mediators. In

Key messages**What is the key question?**

- Could targeting the tetrahydrobiopterin system attenuate pulmonary artery remodelling in pulmonary fibrosis?

What is the bottom line?

- Tetrahydrobiopterin (BH4) is downregulated in plasma and pulmonary arteries from patients with idiopathic pulmonary fibrosis. Stimulation of the BH4 biosynthesis 'salvage pathway' by oral administration of sepiapterin reduced pulmonary remodelling and pulmonary fibrosis in a bleomycin-induced pulmonary fibrosis animal model and inhibited the endothelial-to-mesenchymal transition as a source of myofibroblasts in human pulmonary artery endothelial cells.

Why read on?

- The results suggest that targeting the BH4 synthesis 'salvage pathway' may be a new therapeutic strategy to attenuate pulmonary hypertension in idiopathic pulmonary fibrosis.

the early stages, vascular disease is affected by muscularisation followed by fibrous vascular atrophy and pronounced intimal fibrosis. Subsequently, there is fibrous atrophy of the media and, finally, fibrous ablation of affected vessels. Perivascular fibrosis may influence the distension of the pulmonary vessels, possibly augmenting pulmonary vascular resistance and pulmonary artery pressure.² The blood vessels may themselves participate in the genesis of IPF, and similar cytokine disruptions have been described in IPF and pulmonary hypertension including changes in levels of transforming growth factor β (TGF- β), connective tissue growth factor (CTGF) or endothelin-1 (ET-1). This suggests that these disorders share pathogenic features and that one may influence, generate or perpetuate the other.

The various cellular processes involved in pulmonary artery remodelling are observed in pulmonary hypertension-associated IPF, including endothelial dysfunction,³ endothelial-to-mesenchymal transition as a source of fibroblasts,⁴ as well as fibroblast and pulmonary artery smooth muscle proliferation and transition to myofibroblasts.⁵ Dysfunction of

pulmonary artery endothelial cells is present in IPF³ and may manifest as enhanced synthesis of ET-1, TGF- β , reactive oxygen/nitrogen species and platelet-derived growth factor⁶ or decreased synthesis of vasodilators and anti-smooth muscle cell proliferation molecules such as nitric oxide (NO) or prostacyclin.⁷

NO is synthesised by three distinct nitric oxide synthases (NOS), two of which are expressed constitutively in neurons (nNOS) and vascular endothelial cells (eNOS). The expression of a third isoform (iNOS) is induced by a number of cytokines in a broad spectrum of cell types.⁸ NO bioavailability is reduced in pulmonary hypertension due to reduced NO synthesis or increased NO consumption by reactive oxygen species. All three NOS isoforms additionally require tetrahydrobiopterin (BH4) for their catalytic activity.⁸ Thus, when BH4 levels are adequate, NOS produces NO; low levels of BH4 cause uncoupled NOS enzymatic activity, generating NO, superoxide and peroxynitrite, thus contributing to vascular oxidative stress and endothelial dysfunction. BH4 bioavailability is determined by the balance between de novo synthesis and oxidative degradation to non-active BH2. GTP cyclohydrolase 1 is the first step and rate-limiting enzyme for de novo BH4 biosynthesis. An alternative 'salvage pathway' transforms exogenous sepiapterin to BH4 through the enzyme sepiapterin reductase.⁹

Pulmonary artery expression of eNOS is decreased or absent in the endothelium of patients with IPF while iNOS is highly expressed, in parallel with an increase in reactive oxygen species and nitrotyrosine, in the lung tissue of these patients, which suggests uncoupled NOS activity.¹⁰ Recent studies have shown that BH4 or its precursor sepiapterin possesses antioxidant and anti-fibrotic properties in cardiovascular diseases.^{11 12} However, the role of the BH4 system in IPF, as well as the associated pulmonary hypertension, is currently unknown. Based on these observations, we hypothesise that: (1) levels of BH4 in patients with IPF are downregulated by alteration of the enzymes required for BH4 biosynthesis, thus increasing uncoupled NOS and oxidative

stress; (2) oral administration of sepiapterin as a source of intracellular BH4 may improve pulmonary hypertension and lung fibrosis in a model of bleomycin-induced lung fibrosis; and (3) endothelial-to-mesenchymal transition as a source of pulmonary fibroblasts is inhibited by sepiapterin in vitro in cultured pulmonary artery endothelial cells.

METHODS

Details of the methods are shown in the online supplement.

Patients with IPF

Fibrotic lung samples were obtained at lung transplantation surgery or by open lung biopsy for histological diagnosis of the disease. Age-matched normal control lungs were collected from a non-involved segment remote from the solitary lesion of patients undergoing thoracic surgery for removal of a primary lung tumour.

Animal model

Animal studies were performed in accordance with the guidelines of the Committee of Animal Ethics and Well-being of the University of Valencia. Wistar rats were instilled on day 1 with a single intratracheal dose of 3.75 U/kg bleomycin. Sham-treated rats received an identical volume of intratracheal saline instead of bleomycin. Twice daily oral doses of sepiapterin (10 mg/kg) were administered via an intra-oesophageal cannula from day 1 to 21. At the end of the treatment period (day 21) the rats were killed. Right ventricular hypertrophy was measured as described previously.¹³ Right ventricular systolic pressure (RVSP) was determined by right heart catheterisation.

Histological, immunohistochemical and immunofluorescence studies

The severity of lung fibrosis was scored on a scale from 0 (normal lung) to 8 (total fibrotic obliteration of fields) according

Table 1 Clinical characteristics

	Control subjects in lung tissue studies (n=21)	Control subjects in plasma studies (n=30)	IPF patients in lung tissue studies (n=17)	IPF patients in plasma studies (n=36)
Age (years)	66 (53–78)	67 (48–75)	64 (56–75)	63(55–72)
Sex (M/F)	15/6	20/10	12/5	25/11
Smoking				
Never smoked/smokers	9/12	8/22	5/12	6/30
Pack-years	26 (0–32)	24 (0–29)	27.5 (0–32)	30 (0–38)
FEV ₁ , pred	95.2 (90–104)	96 (93–105)	73.7 (58–103)	72 (50–102)
FVC, % pred	96 (93–106)	98.4 (94–105)	72.2 (63–98)	74 (48–92)
TLC, % pred	95 (92–105)	96 (91–107)	73.5 (45–89)	66 (43–90)
Tlco, % pred	94.2 (91–107)	97 (92–107)	50.4 (32–61)	40.5 (20–63)
Ground glass %	0	ND	15 (5–40)	10 (5–30)
Honeycombing %	0	ND	28 (10–40)	25 (12–35)
Pao ₂ , mm Hg	94 (84–100)	96 (85–100)	65 (45–88)	60 (40–85)
mPAP mm Hg/L/min	ND	ND	38.5 (34–44)	43 (36–48)
Steroid (y/n)	0/21	0/30	1/15	12/15
Azathioprine (y/n)	0/21	0/30	4/17	6/36
NAC (y/n)	0/21	0/30	14/17	28/36
Pirfenidone (y/n)	0/21	0/30	4/17	8/36

Data are shown as median (IQR).

Steroid/azathioprine/pirfenidone refers to patients who received this treatment at the time of pulmonary biopsy.

% pred, % predicted; Tlco, transfer factor of the lung for carbon monoxide; FEV₁, forced expiratory volume in 1 s; FVC, forced vital capacity; ground glass %, percentage of pulmonary parenchyma with ground glass in CT image; honeycombing %, percentage of pulmonary parenchyma with honeycombing in CT image; IPF, idiopathic pulmonary fibrosis; mPAP, mean pulmonary artery pressure; NAC, N-acetyl-L-cysteine; ND, not determined; pack-year, 1 year of smoking 20 cigarettes per day; Pao₂, oxygen tension in arterial blood; TLC, total lung capacity.

to the Ashcroft scoring system.¹⁴ Pulmonary artery wall thickness was determined as reported previously.¹⁵ For immunohistochemical analysis of rat and human lungs, sections were immunostained with α -smooth muscle actin, sepiapterin reductase, GTP cyclohydrolase 1, eNOS and iNOS antibodies. Staining intensities of the various antibodies were scored and summed to obtain a composite score of 0–12, as described previously.¹⁶ Immunofluorescence of CD31, collagen type I, α -smooth muscle actin and vascular endothelial (VE)-cadherin was assessed in human pulmonary artery endothelial cells.

Determination of BH4/BH2, nitrites and nitrotyrosine

BH4 and BH2 in plasma, pulmonary artery tissue and cell culture supernatant were measured by high-performance liquid chromatography. NO and nitrotyrosine concentrations were determined using a commercially available ELISA (see online supplement for details).

Isolation of human pulmonary artery endothelial cells

Cell culture experiments were performed using human pulmonary artery endothelial cells isolated from the pulmonary arteries of normal lungs using a commercially available Dynabeads CD31 endothelial cell kit (DynaL Biotech, Germany).

Quantitative PCR and western blotting

Transcript levels were quantified using the $2^{-\Delta\Delta Ct}$ method. Western blotting was used to detect changes in TGF- β 1, ET-1 and phosphorylated Smad3 (p-Smad3) levels in lung tissue and human pulmonary artery endothelial cells.

DCF fluorescence measurement of reactive oxygen species

H₂DCF-DA (2',7'-dichlorodihydrofluorescein diacetate; Molecular Probes, Nottingham, UK) was used to monitor intracellular reactive oxygen species in human pulmonary artery endothelial cells.

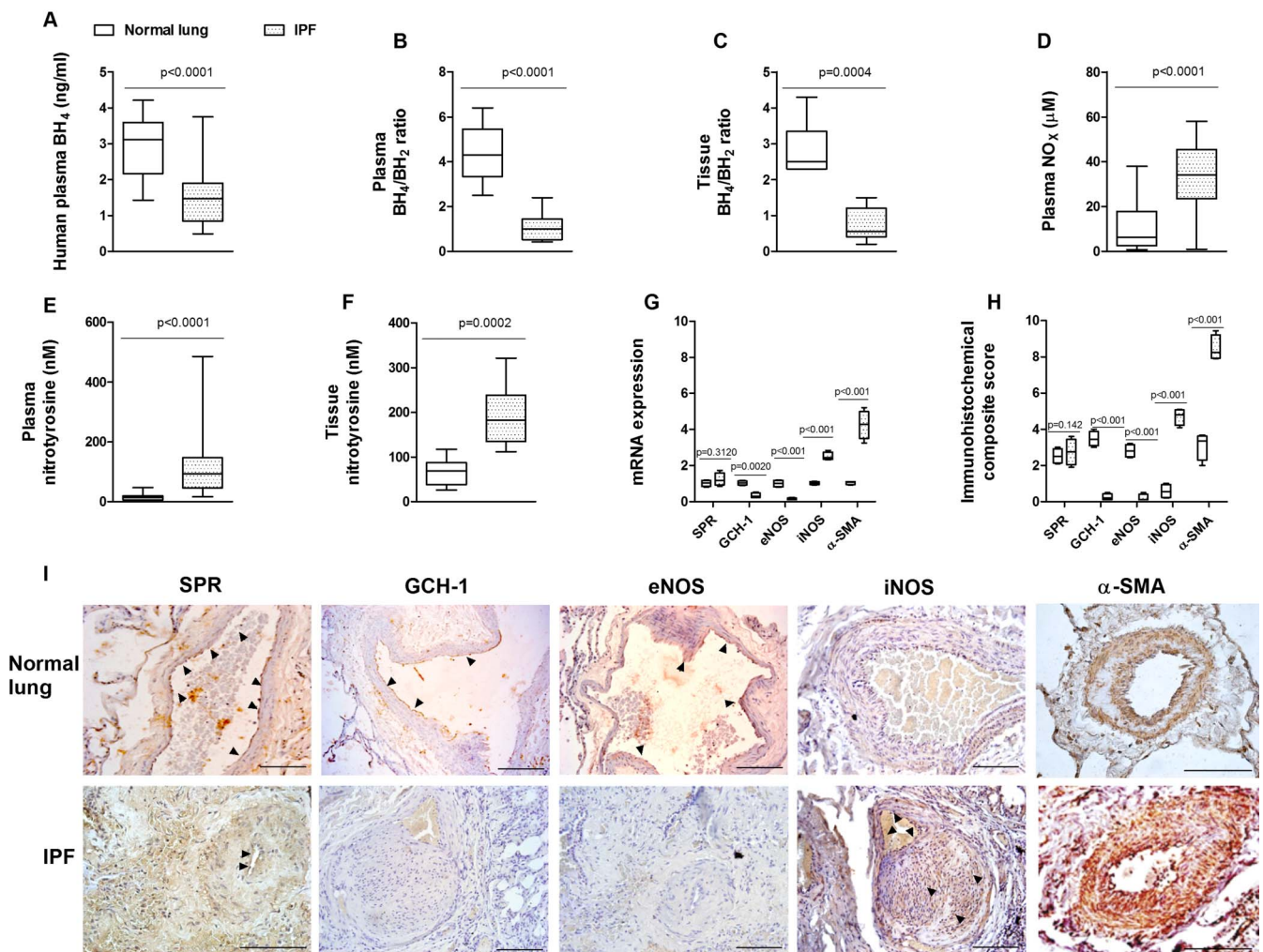


Figure 1 Tetrahydrobiopterin (BH4) bioavailability in idiopathic pulmonary fibrosis (IPF). (A) Plasma BH4 levels, (B) plasma BH4/dihydrobiopterin (BH2) levels, (C) pulmonary artery tissue BH4/BH2 levels, (D) plasma nitrites+nitrates (NO_x), (E) plasma nitrotyrosine, (F) pulmonary artery tissue levels of BH4 in healthy subjects (n=30) and patients with IPF (n=36), (G) expression of sepiapterin reductase (SPR), GTP cyclohydrolase 1 (GCH-1), endothelial nitric oxide synthase (eNOS), inducible nitric oxide synthase (iNOS) and α -smooth muscle actin (α -SMA) genes in pulmonary arteries from 21 normal controls and 17 patients with IPF. Data are expressed as ratios to GAPDH mRNA levels. The box plot in (F) represents the composite score of SPR, GCH-1, eNOS, iNOS and α -SMA markers across pulmonary arteries in 10 slices per patient. Data are presented as a box and whisker plot of medians, IQR and minimum and maximum values. p Values were obtained by Mann–Whitney test. (H, I) Immunohistochemistry of pulmonary arteries. Pulmonary artery sections from normal lungs (n=21) and patients with IPF (n=17) were immunostained for SPR, GCH-1, eNOS, iNOS and α -SMA (brown) and counterstained with haematoxylin. Black arrows show positively immunostained regions. Representative immunohistochemistry images are shown. Scale bar=100 μ m. The IgG isotype control was negative.

Statistical analysis

Statistical analysis was carried out by parametric (animal and cell culture studies) or non-parametric (human studies) analysis, as appropriate; $p < 0.05$ was considered to indicate statistical significance. For non-parametric tests, data are displayed as medians, IQR and minimum and maximum values analysed by the Mann–Whitney test. Parametric data are expressed as means \pm SE of n experiments using the Student t test or one-way or two-way analysis of variance followed by the Bonferroni post hoc test.

RESULTS

Bioavailability of BH4 in patients with IPF

Both controls and patients with IPF were prospectively recruited from 2008 to 2012. Clinical data from enrolled patients are shown in table 1. Levels of BH4 were significantly downregulated in plasma from patients with IPF (1.46 ± 0.69 ng/mL) compared with healthy controls (2.93 ± 0.8 ng/mL; figure 1A). Additionally, BH4/BH2 was lower in plasma and pulmonary artery tissue from patients with IPF (figure 1B,C). Plasma levels of NO_x (nitrate and nitrite) were increased in patients with IPF compared with healthy subjects (figure 1D). Increased levels of plasma and pulmonary artery tissue nitrotyrosine were also observed in patients with IPF compared with healthy subjects (figure 1E,F). In contrast to control normal lungs, pulmonary arteries from patients with IPF showed a lack of gene and protein expression of GTP cyclohydrolase 1 and eNOS, while

iNOS and α -smooth muscle actin expression was upregulated in pulmonary arteries (figure 1G–I). However, the expression of sepiapterin reductase was similar in pulmonary arteries from control subjects and patients with IPF. No correlation between clinical data or pulmonary hypertension with BH4 values was identified in patients with IPF.

Effects of sepiapterin on bleomycin-induced lung fibrosis and mortality

Following 21 days of intratracheal bleomycin instillation, a marked loss of body weight and an increase in lung mass and mortality were observed (figure 2A–C). Twice daily oral administration of sepiapterin (10 mg/kg) reduced body weight loss and increased lung mass secondary to fibrosis, and increased survival. Bleomycin induced a fibrotic response in the lung, with enhanced expression of fibrotic markers TGF- β 1, ET-1, CTGF and collagen type I (figure 2D) and increased deposition of collagen, as visualised by Masson's trichrome staining (figure 2E). Sepiapterin alleviated histologically observed multifocal fibrotic lesions, resulting in fewer organised and smaller foci and reduced septal enlargement with a diminished Ashcroft fibrosis score (figure 2F).

Sepiapterin improves bleomycin-induced pulmonary remodelling

Right ventricular hypertrophy (RV/LV+septum) and pulmonary vascular remodelling developed following bleomycin treatment

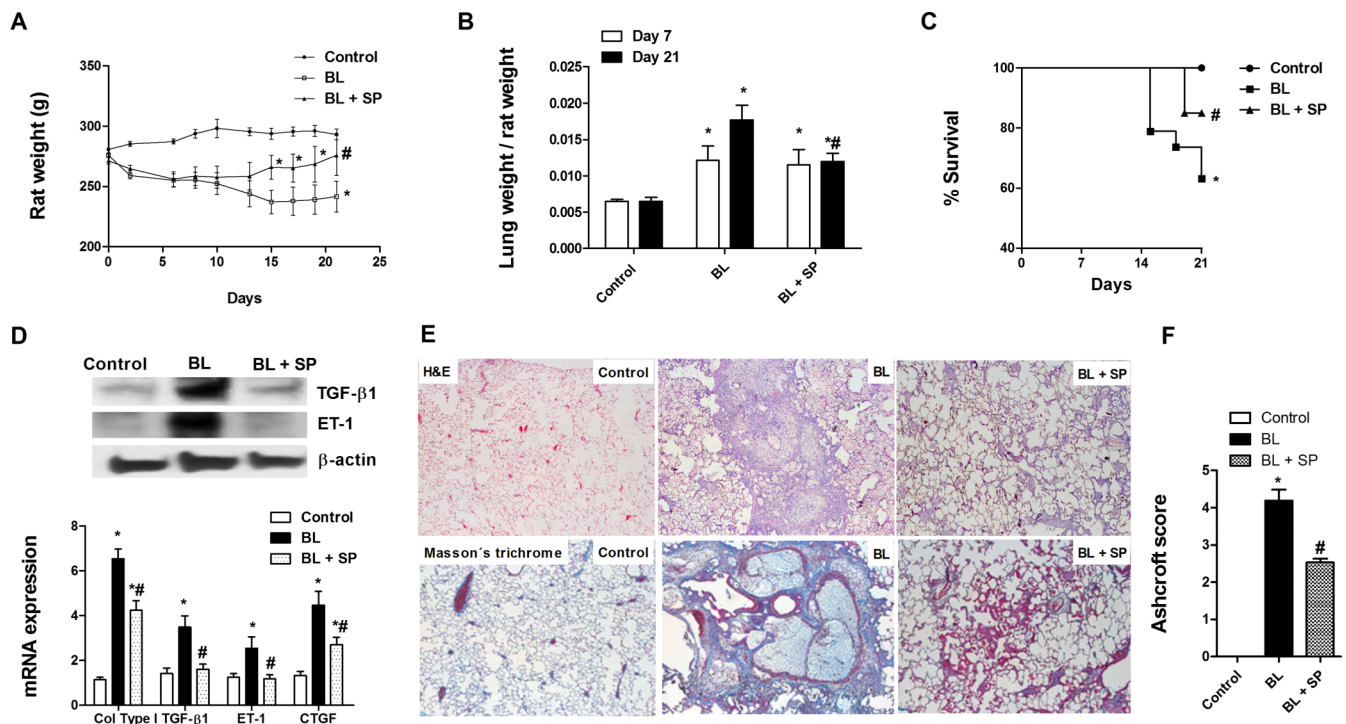


Figure 2 Sepiapterin improves bleomycin-induced pulmonary fibrosis. Wistar rats received a single intratracheal dose of bleomycin (BL; 3.75 U/kg) on day 1. Sepiapterin (SP; 10 mg/kg twice daily orally) or vehicle was administered from day 1 until analysis at day 21 ($n=10$ per group). (A) Rat weight and (B) lung mass were monitored for 21 days. (C) Kaplan–Meier survival curve showing 60% survival over the 21-day BL period (square), 83% in the SP-treated group (triangle) and 100% in the control rat group (circle); $*p < 0.05$, log-rank test. (D) Total lung protein and gene expression of the profibrotic markers transforming growth factor β 1 (TGF- β 1), endothelin 1 (ET-1), collagen type I (col type I) and connective tissue growth factor (CTGF). Data are expressed as ratios to GAPDH mRNA levels and to β -actin protein levels, normalised to the control group. (E) Representative western blot images of total TGF- β 1 and ET-1; H&E staining (upper panels, 40 \times) and Masson's trichrome (lower panels, 40 \times); collagen stained in blue) of controls, BL and BL+SP. (F) Fibrosis Ashcroft scores were assessed as described in the Methods section. Results are expressed as means \pm SE ($n=10$). Statistical significance was assessed using a t test or one-way analysis of variance followed by a Bonferroni post hoc test. $*p < 0.05$ vs control, $\#p < 0.05$ vs BL.

(figure 3A,B). By day 21, pulmonary hypertension was observed in the bleomycin group, as peak RVSP had increased from 19.8 ± 4.2 mm Hg in control rats to 42.12 ± 5.1 mm Hg in the bleomycin group (figure 3C). Sepiapterin suppressed RV hypertrophy almost completely, pulmonary vascular remodelling and

normalised pulmonary hypertension to 20.9 ± 4.7 mm Hg at day 21. Sepiapterin also reduced collagen deposition visualised by Masson's trichrome staining and muscularisation visualised by α -smooth muscle actin immunostaining in the walls of the pulmonary arteries (figure 3D).

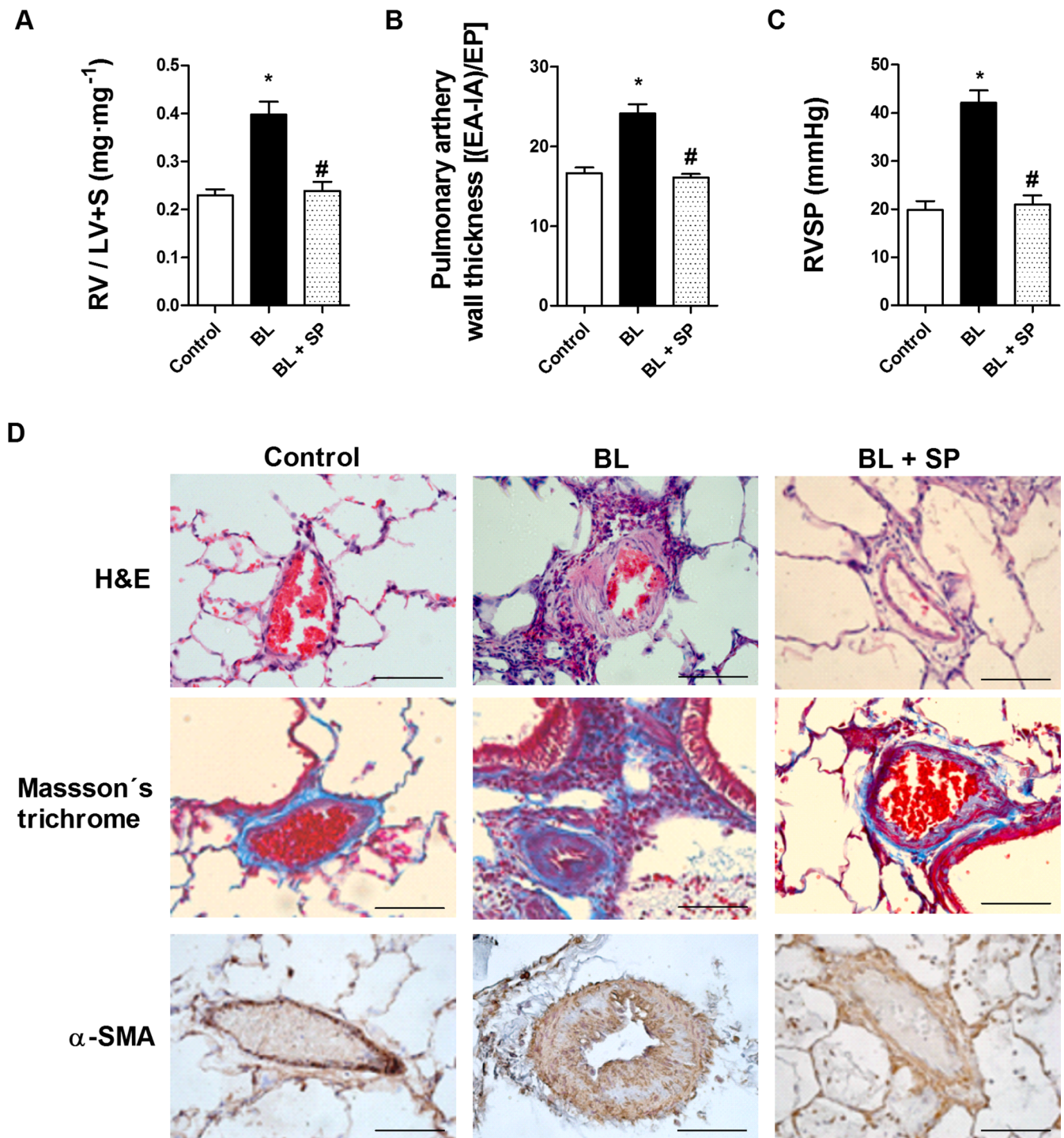


Figure 3 Analysis of bleomycin-induced pulmonary vascular remodelling and right ventricular hypertrophy. Rats received a single intratracheal dose of bleomycin (BL; 3.75 U/kg) on day 1. Sepiapterin (SP; 10 mg/kg twice daily orally) or vehicle was administered from day 1 until analysis at day 21 (n=10 per group). (A) Right ventricular hypertrophy (expressed as RV/LV+S ratio). (B) Pulmonary artery wall thickness was calculated by dividing the wall area (EA-IA) by the external perimeter (EP) in intra-acinar pulmonary arteries immunostained with α -smooth muscle actin (α -SMA) antibody. (C) Right ventricular systolic pressure (RVSP; mm Hg) in control rats, BL and BL+SP 21 days after BL instillation. (D) H&E staining (upper panels), scale bar=20 μ m) and Masson's trichrome (lower panels, collagen stained in blue) of controls, BL and BL+SP. Results are expressed as means \pm SE (n=10). Statistical significance was assessed using one-way analysis of variance followed by a Bonferroni post hoc test. *p<0.05 vs control, #p<0.05 vs BL.

Effects of sepiapterin on BH4 and NO bioavailability in bleomycin-treated rats

Absolute plasma levels of BH4 at day 21 were significantly downregulated in the bleomycin group (figure 4A). Decreased levels of BH4 were accompanied by an increase in partially oxidised BH2 levels, so the plasma BH4/BH2 ratio was decreased in the bleomycin group (figure 4B). In plasma from untreated rats the NOx concentration was significantly lower than in bleomycin-treated rats (control $9.2 \pm 2.5 \mu\text{M}$ vs bleomycin $19.5 \pm 5.3 \mu\text{M}$; figure 4C). Additionally, plasma levels of nitrotyrosine were increased approximately twofold over control rats (figure 4D). Oral administration of sepiapterin increased plasma BH4 as well as BH4/BH2 to levels similar to control rats (figure 4A,B). Sepiapterin inhibited bleomycin-induced upregulation of plasma NOx and nitrotyrosine to levels similar to those of control rats (figure 4C,D). Immunohistochemical analysis of pulmonary arteries showed a significant decrease in GTP

cyclohydrolase 1 expression (figure 4E,F), but no change in sepiapterin reductase, after 21 days of bleomycin exposure. In control rats, eNOS expression was located primarily in endothelial cells while, in the bleomycin group, eNOS expression was not observed. In contrast, iNOS was highly induced in pulmonary arteries of bleomycin-treated rats. Oral administration of the sepiapterin reductase substrate sepiapterin to bleomycin-treated rats significantly increased GTP cyclohydrolase 1 and eNOS expression and partially inhibited iNOS induction in pulmonary arteries (figure 4E,F).

Sepiapterin inhibits the endothelial-to-mesenchymal transition induced by fibrotic mediators

Human pulmonary artery endothelial cells isolated from pulmonary arteries of normal lungs were stimulated with TGF- β 1 (5 ng/mL) or ET-1 (100 nM) for 72 h. Both TGF- β and ET-1 elicited an increase in levels of the mesenchymal markers α -smooth

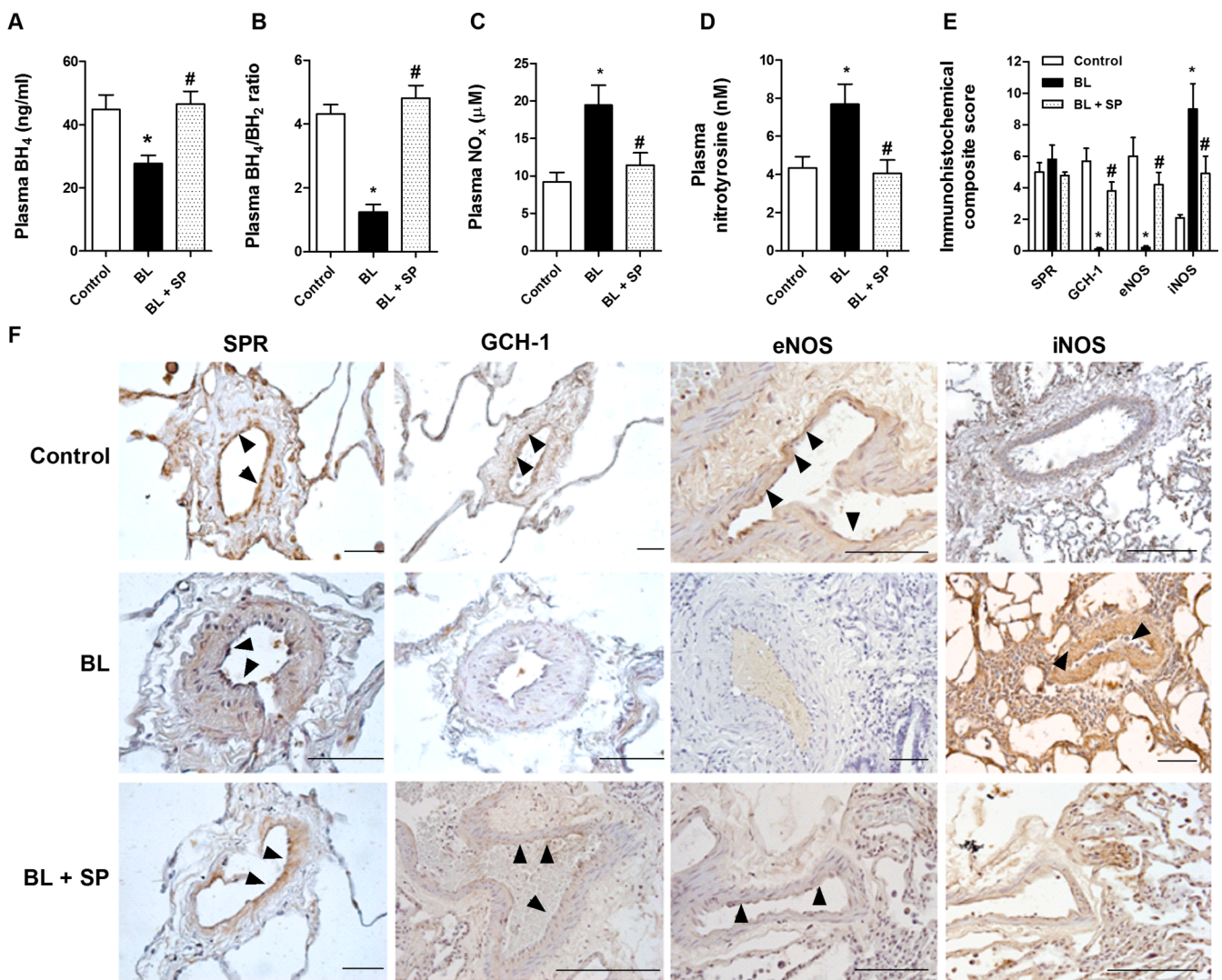


Figure 4 Sepiapterin increases tetrahydrobiopterin (BH4) and reduces nitrotyrosine plasma levels in bleomycin-treated rats. Rats received a single intratracheal dose of bleomycin (BL; 3.75 U/kg) on day 1. Sepiapterin (SP; 10 mg/kg twice daily orally) or vehicle was administered from day 1 until analysis at day 21 (n=10 per group). (A) BH4 levels, (B) BH4/dihydrobiopterin (BH2), (C) nitrites+nitrates (NOx), (D) nitrotyrosine rat plasma levels (n=10 per group). (E, F) Immunohistochemistry of pulmonary arteries from control vehicle, BL and BL+SP groups were immunostained for sepiapterin reductase (SPR), GTP cyclohydrolase 1 (GCH-1), endothelial nitric oxide synthase (eNOS) and inducible nitric oxide synthase (iNOS) (brown) and counterstained with haematoxylin. Black arrows show positively immunostained regions. Representative immunohistochemistry images are shown. Scale bar=50 μm . The IgG isotype control was negative. The box plot in (E) represents the composite score of SPR, GCH-1, eNOS and iNOS markers across the pulmonary arteries in 10 slices per animal. Results are expressed as means \pm SE (n=10). Statistical significance was assessed using one-way analysis of variance followed by a Bonferroni post hoc test. *p<0.05 vs control, #p<0.05 vs BL.

muscle actin, SM22- α and its transcriptional regulators snail and slug after 72 h. Similarly, α -smooth muscle actin protein immunofluorescence was also upregulated. In contrast, the endothelial markers CD31, VE-cadherin and vascular endothelial growth factor receptor were downregulated, supporting a change in phenotype (figure 5A–F). Sepiapterin pretreatment dose-dependently inhibited the upregulation of mesenchymal markers and downregulation of endothelial markers induced by both TGF- β 1 and ET-1 (figure 5A–F). In other experiments, sepiapterin dose-dependently inhibited intracellular reactive oxygen species formation following TGF- β 1 or ET-1 stimulation (figure 6A,B). Furthermore, sepiapterin suppressed TGF- β 1- and ET-1-induced Smad3 phosphorylation. The antioxidant N-acetyl-L-cysteine also suppressed Smad3 phosphorylation (figure 6C). ET-1-induced Smad3 phosphorylation was inhibited by blocking active TGF- β 1 in the supernatant with the monoclonal antibody (mAb)-TGF- β 1 (figure 6D). As observed for sepiapterin, N-acetyl-L-cysteine and SIS3, an inhibitor of Smad3, inhibited the increase in levels of mesenchymal markers and decrease in endothelial markers induced by TGF- β 1 and ET-1 (figure 6E–H). TGF- β 1 and ET-1 decreased eNOS expression and NOx in cell supernatants (figure 7A–C), which were inhibited by sepiapterin and N-acetyl-L-cysteine. iNOS expression was upregulated in endothelial cells following TGF- β 1 and ET-1 stimulation and inhibited by sepiapterin and N-acetyl-L-cysteine. TGF- β 1 and ET-1 also suppressed GTP cyclohydrolase 1 expression but did not affect sepiapterin reductase (figure 7A,B), and sepiapterin and N-acetyl-L-cysteine prevented GTP cyclohydrolase 1 downregulation. The addition of mAb-TGF- β 1 rescued ET-1-induced eNOS and GTP cyclohydrolase 1 downregulation and normalised iNOS expression. Moreover, extracellular nitrotyrosine levels were

increased in response to TGF- β 1 and ET-1 while culture supernatant levels of BH4, as well as BH4/BH2, were downregulated (figure 7D–F). Sepiapterin administration suppressed nitrotyrosine levels and increased BH4 and BH4/BH2 to near control values (figure 7D–F).

Sepiapterin inhibits the endothelial-to-mesenchymal transition in vivo

Pulmonary artery sections immunostained with α -smooth muscle actin and VE-cadherin showed an endothelial layer marked with VE-cadherin in control rats and with α -smooth muscle actin and VE-cadherin in bleomycin-treated rats. Oral administration of sepiapterin to bleomycin-treated rats showed an endothelial layer marked by VE-cadherin, suggesting inhibition of endothelial-to-mesenchymal transition in vivo (figure 8). In contrast to normal human pulmonary arteries, those from patients with IPF showed immunostaining with CD31 and collagen type I or with α -smooth muscle actin and VE-cadherin in endothelial cells, as well as in the intima, suggesting a role for endothelial-to-mesenchymal transition in pulmonary remodelling.

DISCUSSION

In this study we provide new evidence of the role of the BH4 system in pulmonary hypertension-associated IPF. BH4, the cofactor of NOS, was decreased in plasma from patients with IPF, contributing to uncoupled NOS activity and an increase in oxidative stress and nitrotyrosine expression. Because pulmonary artery sepiapterin reductase levels were not affected in IPF, oral administration of sepiapterin increased levels of BH4 coupling NOS to produce NO but not peroxynitrite, thereby

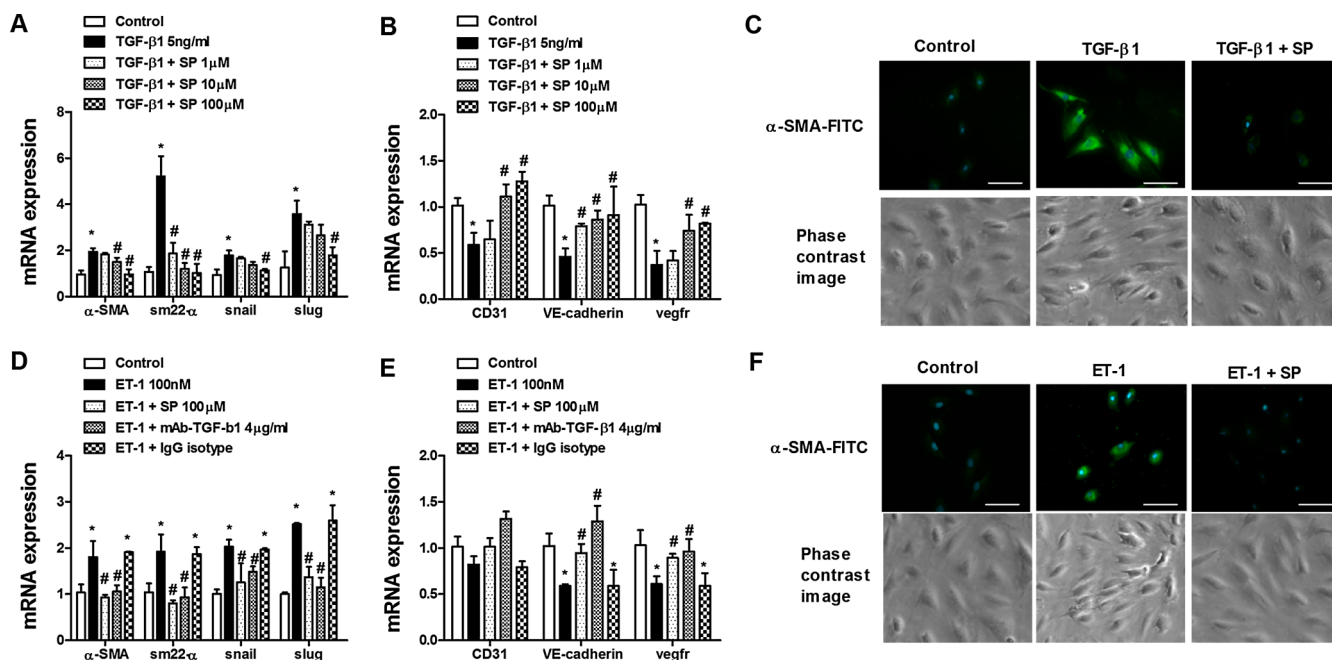


Figure 5 Sepiapterin inhibits endothelial-to-mesenchymal transition in human pulmonary artery endothelial cells (HPAECs). HPAECs were isolated from normal lungs. Cells were incubated with sepiapterin (SP; 1–100 μ M) for 30 min before stimulation with (A–C) transforming growth factor β 1 (TGF- β 1; 5 ng/mL) or (D–F) endothelin 1 (ET-1; 100 nM) for 72 h. Total RNA was isolated for real-time PCR analysis. TGF- β 1 and ET-1 upregulated mRNA expression of mesenchymal markers α -smooth muscle actin (α -SMA), SM22- α , slug and snail and downregulated mRNA expression of the vascular endothelial markers CD31, vascular endothelial (VE)-cadherin and vascular endothelial growth factor receptor (VEGFR). (D, E) The addition of mAb-TGF- β 1 effectively inhibited the ET-1-induced increase in mesenchymal marker expression and the decrease in vascular endothelial marker expression. (C, F) Phase contrast images and immunofluorescence staining of α -SMA-FITC and DAPI (blue indicates nuclei). Representative images are shown. Scale bar=5 μ m. Data are expressed as ratios to GAPDH mRNA normalised to the solvent control group. Results are expressed as means \pm SE of 3–5 (four cell control population) experiments per condition. Two-way analysis of variance followed by post hoc Bonferroni tests. *p<0.05 vs solvent controls; #p<0.05 vs stimulus.

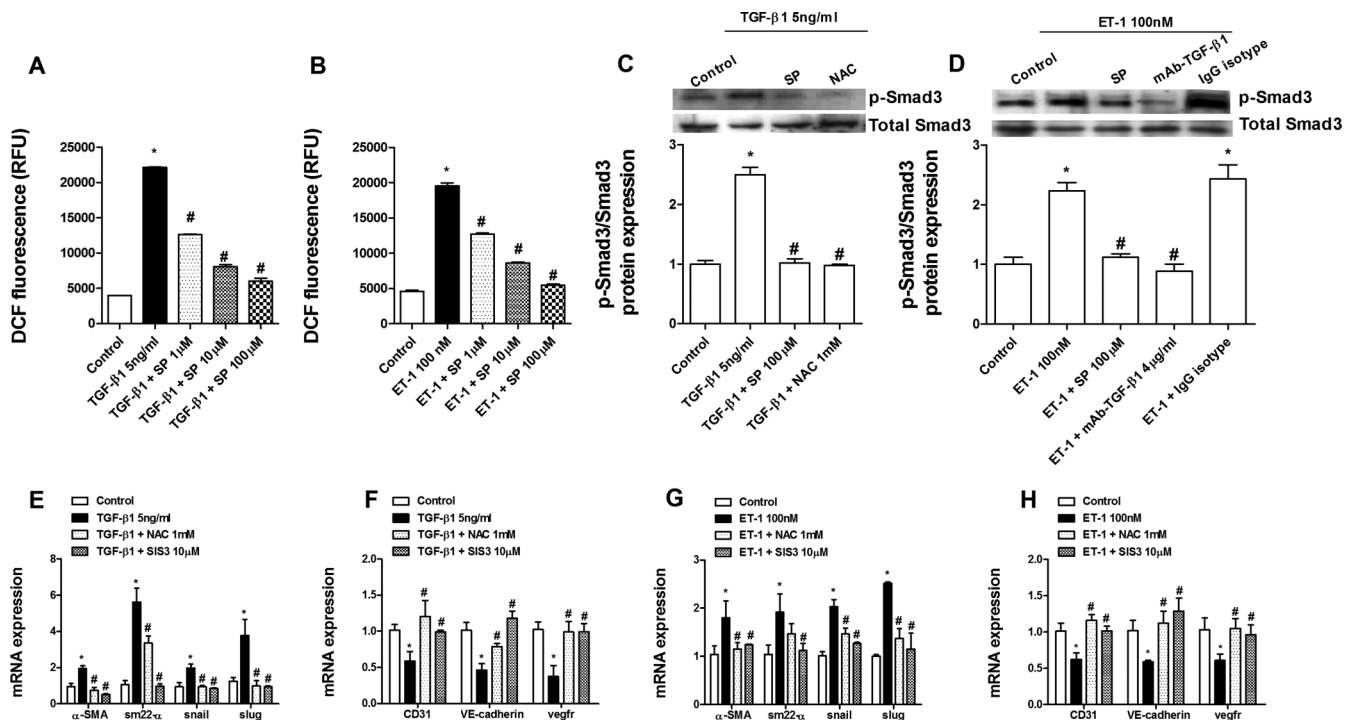


Figure 6 Sepiapterin inhibition of endothelial-to-mesenchymal transition is mediated by a reduction in reactive oxygen species levels and phosphorylation of Smad3. Human pulmonary artery endothelial cells were incubated with sepiapterin (SP; 1–100 μ M), the antioxidant N-acetyl-L-cysteine (NAC; 1 mM) or the inhibitor of Smad3 (SIS3; 10 μ M) for 30 min before stimulation with transforming growth factor β 1 (TGF- β 1; 5 ng/mL) or endothelin 1 (ET-1; 100 nM) stimulation for (A, B) 30 min, (C, D) 60 min, or (E–H) 72 h. (A, B) Reactive oxygen species were determined by means of DCF fluorescence intensity (in relative fluorescence units (RFU) after TGF- β 1 or ET-1 stimulation in the presence or absence of SP. (C, D) TGF- β 1 or ET-1 increased the phosphorylation of Smad3 that was inhibited by SP, NAC and mAb-TGF- β 1. Phospho-Smad3 and protein levels were expressed as ratios to total Smad3 and normalised to the control group. Representative western blot images are shown (n=4). (E–H) NAC and SIS3 inhibited (E, F) TGF- β 1-induced and (G, H) ET-1-induced upregulation of mesenchymal markers and downregulation of endothelial markers. Data in (E–H) are expressed as ratios to GAPDH mRNA levels and normalised to the solvent control group. Results are expressed as means \pm SE of n=3–5 (four-cell control population) experiments per condition. Two-way analysis of variance followed by post hoc Bonferroni tests. *p<0.05 vs solvent controls; #p<0.05 vs stimulus.

decreasing pulmonary hypertension and lung fibrosis in bleomycin-treated rats. Furthermore, endothelial-to-mesenchymal transition as a source of fibroblasts was inhibited by sepiapterin in vitro and in vivo. These results provide support for a new therapeutic strategy to attenuate pulmonary hypertension in IPF through the administration of sepiapterin.

The study of NO in IPF lungs is not novel. More than a decade ago Saleh *et al*¹⁰ reported that the lungs of patients with IPF express high levels of iNOS and nitrotyrosine, a product of peroxynitrite, and that eNOS expression was almost absent in the endothelium of pulmonary arteries of patients with IPF, thus contributing to the increased oxidative stress found in IPF. Comparable results were observed in this study. However, oxidative stress in patients with IPF is reportedly not restricted to lung tissue and is also found in serum.¹⁷ We identified high levels of nitrotyrosine in the plasma of patients with IPF, which suggests uncoupled NOS activity. In contrast to eNOS, expression of iNOS leads to a 1000-fold increase in levels of NO which mediates defence and pathological processes.¹⁸ When iNOS is uncoupled, NO formation is decreased in favour of O₂⁻ with which NO reacts rapidly to form peroxynitrite, thus contributing to oxidation. We observed a reduction in plasma BH4 in patients with IPF, which confirmed uncoupled NOS activity. Furthermore, the levels of the BH4 oxidation product BH2 were upregulated. Because BH2 lacks NOS cofactor activity and competes with BH4 for binding to NOS, a decreased ratio of BH4/BH2 is an acceptable measure of uncoupled NOS.¹⁹ Low

levels of BH4 may result from oxidative degradation to BH2 or by defects in enzymatic de novo synthesis. A combination of the two processes was observed in the patients with IPF recruited in this study as the expression of the de novo synthesis enzyme GTP cyclohydrolase 1 was downregulated in pulmonary arteries without changes in sepiapterin reductase.

Unlike the many studies of NOS, there is little evidence of the role of GTP cyclohydrolase 1 and sepiapterin reductase in pulmonary hypertension and no evidence of pulmonary hypertension secondary to IPF. Mice deficient in GTP cyclohydrolase 1/BH4 have pulmonary hypertension without systemic hypertension,²⁰ and a spontaneously hypertensive rat model exhibits decreased GTP cyclohydrolase 1/BH4 and increased sepiapterin reductase expression in the aorta.²¹ In contrast, the administration of sepiapterin restored pulmonary artery endothelial function of fetal lambs with persistent pulmonary hypertension.²² In a similar way, a sepiapterin-based strategy improves post-myocardial infarction fibrosis and left ventricular remodelling by activating the BH4 synthesis 'salvage pathway' and increasing bioavailable NO predominantly derived from iNOS.¹²

Sepiapterin may be a more preferable pharmacological tool than BH4 to investigate the role of NOS uncoupling on pulmonary hypertension and IPF progression because it is a stable precursor of BH4 and is more membrane-permeable than BH4.²³ We have shown here that sepiapterin reductase expression is not altered in pulmonary arteries from patients with IPF, suggesting that the BH4 synthesis 'salvage pathway' remains

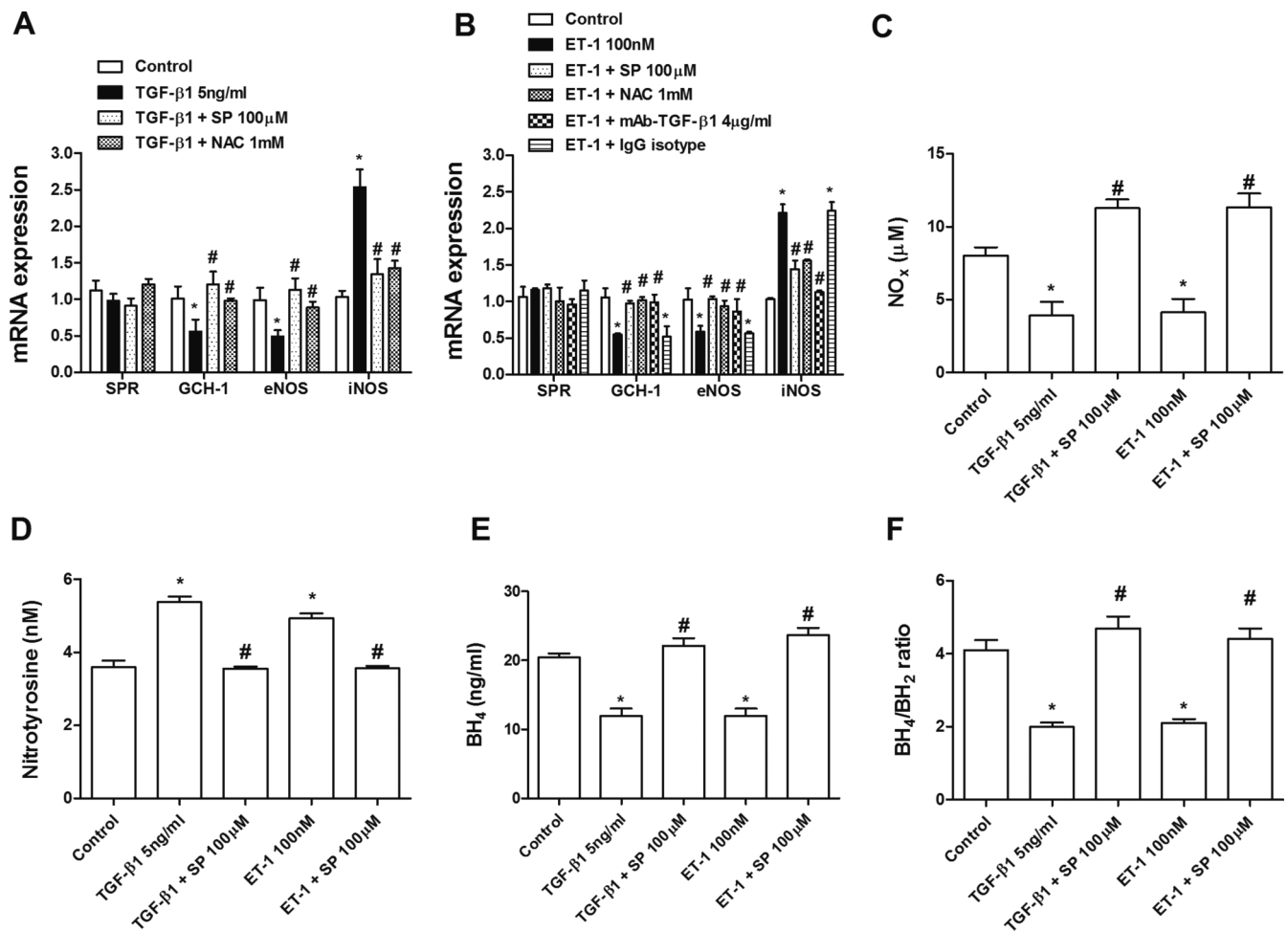


Figure 7 Sepsiperin (SP) improves tetrahydrobiopterin (BH4) bioavailability during endothelial-to-mesenchymal transition. Human pulmonary artery endothelial cells (HPAECs) were incubated with SP (100 μM), N-acetyl-L-cysteine (NAC; 1 mM), mAb-TGF-β1 (4 μg/mL) or with the IgG isotype control for 30 min and stimulated with (A) transforming growth factor β1 (TGF-β1) or (B) endothelin 1 (ET-1) for 72 h. (A, B) Expression of the sepiapterin reductase (SPR), GTP cyclohydrolase 1 (GCH-1), endothelial nitric oxide synthase (eNOS) and inducible nitric oxide synthase (iNOS) genes in HPAECs. Data are expressed as ratios to GAPDH mRNA levels. Culture supernatant levels of (C) nitrites+nitrates (NO_x), (D) nitrotyrosine, (E) BH4 and (F) BH4/BH2 were determined after 72 h of stimulation with TGF-β1 or ET-1 in the presence or absence of SP. Results are expressed as means±SE of n=3–4 (four-cell control population) experiments per condition. Two-way analysis of variance followed by post hoc Bonferroni tests. *p<0.05 vs solvent controls; #p<0.05 vs stimulus.

activated and susceptible to stimulation by exogenous administration of sepiapterin. Recent studies have shown the importance of sepiapterin reductase expression for sepiapterin-induced BH4 levels.²⁴ Based on these observations, we assessed the beneficial effects of oral sepiapterin in a bleomycin-induced pulmonary fibrosis model, an appropriate model of pulmonary hypertension associated with pulmonary fibrosis.²⁵ As observed in humans with IPF, comparable sepiapterin reductase expression was observed in control and bleomycin-instilled rats while GTP cyclohydrolase 1 and eNOS were downregulated in pulmonary arteries. In contrast, iNOS expression was upregulated, as measured by plasma nitrotyrosine and NO_x, suggesting uncoupled NOS. This was confirmed by the reduction in BH4 plasma levels. Supporting the hypothesis that the ‘salvage pathway’ remains activated in pulmonary fibrosis, oral administration of sepiapterin improved pulmonary artery remodelling and hypertension, RV hypertrophy, lung fibrosis extension and rat survival. These events occurred concurrently with coupled NOS function through an increase in BH4/BH2 and a reduction of plasma nitrotyrosine levels, which support similar findings in a mouse model of myocardial

infarction.¹² However, despite the frequent use of the bleomycin model of pulmonary fibrosis, it has significant limitations in its ability to mimic human IPF since many treatments successful in the bleomycin model were not transferable to human IPF.

To explore possible mechanisms associated with sepiapterin treatment, we studied key molecules related to both pulmonary hypertension and pulmonary fibrosis such as TGF-β1 and ET-1. TGF-β1 and ET-1 share pathological activities in pulmonary hypertension and IPF, such as increasing the profibrotic markers collagen type I or CTGF or inducing fibroblast/myofibroblast transformation. Thus, both TGF-β1 and ET-1 are implicated in the cellular processes of epithelial-to-mesenchymal transition,^{26–27} endothelial-to-mesenchymal transition,^{28–29} fibroblast and smooth muscle proliferation and myofibroblast transformation,⁵ and in vascular and lung tissue remodelling of patients with IPF. Notably, oral sepiapterin administration inhibited TGF-β1 and ET-1 expression, suggesting an important role in cellular fibroblast-like transformation. Particularly important is the role of NO in cellular transformation. Inhaled NO attenuated extracellular matrix accumulation and the number of lung myofibroblasts and improved endothelial function in patients

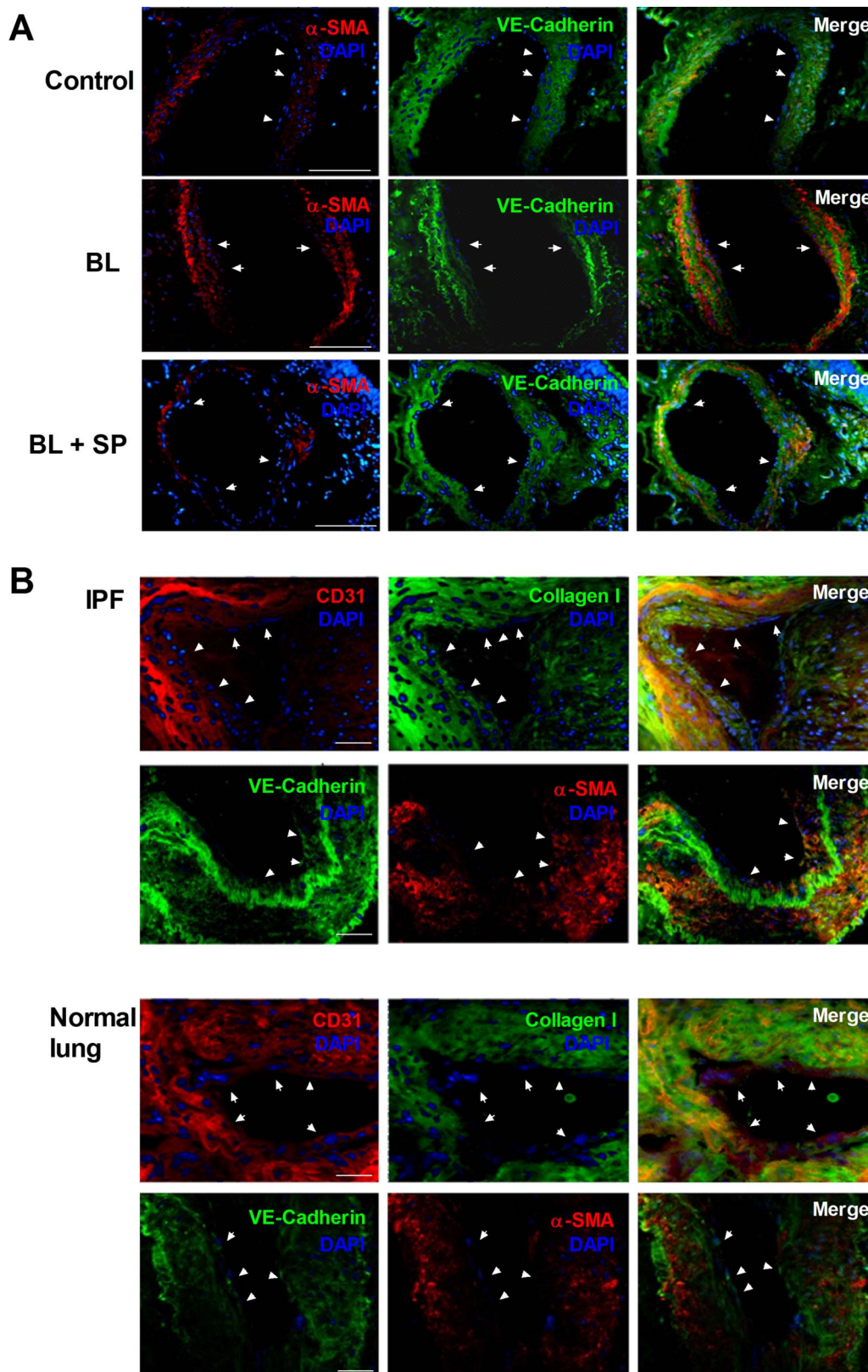


Figure 8 Endothelial-to-mesenchymal transition occurs in fibrotic lungs in vivo. Photomicrographs of representative histological sections from (A) pulmonary rat tissue of the control, bleomycin (BL; 3.75 U/kg intratracheally at day 1) and bleomycin plus sepiapterin (BL + SP; 10 mg/kg twice daily orally) groups (n=6) or (B) pulmonary human tissue from normal lungs (n=6) or idiopathic pulmonary fibrosis (IPF) lungs (n=10). Tissue sections were immunostained with CD31, vascular endothelial (VE)-cadherin, collagen type I or α -smooth muscle actin (α -SMA) antibodies followed by anti-mouse rhodamine or anti-rabbit-FITC secondary antibodies and 4',6-diamidino-2-phenylindole (DAPI) to stain nuclei. Representative images are shown. White arrows indicate pulmonary artery endothelial cells. IgG isotype controls were negative. Scale bar=30 μ m (panel A) or 150 μ m (panel B).

with IPF with pulmonary hypertension.³ In addition, TGF- β 1-induced alveolar epithelial-to-mesenchymal transition was mediated by downregulation of eNOS/NO and inhibited by increasing NO. In a similar way, chronic eNOS inhibition induces endothelial-to-mesenchymal transition in kidney endothelial cells.³⁰ Recent data demonstrated that, in vivo, pulmonary capillary endothelial cells, through endothelial-to-mesenchymal transition, might serve as a source of fibroblasts in pulmonary fibrosis.⁴ The activity of sepiapterin as an endothelial-to-mesenchymal transition inhibitor may therefore explain its inhibitory effects on pulmonary artery remodelling and lung fibrosis. In this study, TGF- β 1 and ET-1 induced endothelial-to-mesenchymal transition in human pulmonary artery endothelial cells. Endothelial-to-mesenchymal transition induced by TGF- β 1 was mediated by increased Smad3 phosphorylation and intracellular reactive oxygen species generation, which confirms previous observations.^{31 32} ET-1-induced endothelial-to-mesenchymal transition was provoked by the release of TGF- β 1 and its autocrine action, similar to the mechanism underlying ET-1-mediated alveolar epithelial-to-mesenchymal transition.²⁶ As reported previously, TGF- β 1 and ET-1 decreased the expression of eNOS^{30 33} but increased the expression of iNOS, which is consistent with a change in phenotype.³⁴ However, nitrotyrosine levels were upregulated in human pulmonary artery endothelial cells, suggesting uncoupled NOS during the endothelial-to-mesenchymal transition process. These results were corroborated by those showing that GTP cyclohydrolase 1 expression and BH4 levels were also reduced after TGF- β 1 and ET-1 stimulation. As observed in human pulmonary artery endothelial cells from patients with IPF and in lung endothelial cells from bleomycin-induced pulmonary fibrosis, the expression of sepiapterin reductase was not modified. Thus, administration of sepiapterin to human pulmonary artery endothelial cells cultures inhibited TGF- β 1 and ET-1-induced endothelial-to-mesenchymal transition by coupling NOS, decreasing reactive oxygen species and inhibiting phosphorylation of Smad3.

In summary, our findings provide new evidence of the participation of the BH4 system in pulmonary hypertension associated with IPF. Targeting the BH4 synthesis 'salvage pathway' by sepiapterin administration may be a new therapeutic strategy to attenuate pulmonary hypertension in IPF and inhibit IPF progression.

Acknowledgements We thank G Juan and E Guijarro of the Respiratory and Surgery units of the Hospital General, Valencia, Spain for facilitating clinical data and tissue collection.

Contributors PA, JM, JC: conception and design. PA, JM, AD, AS-M, AX, FP-V, AC: acquisition of data. PA, JM, JC: analysis and interpretation of data. JM, AD, AS-M, AX, FP-V, AC, JC: drafting the article or revising it critically for important intellectual content. All authors approved this version of the manuscript.

Funding This work was supported by the Spanish government by grants SAF2011-26443 (to JC), FIS CP11/00293 (to JM), CIBERES (CB06/06/0027), ADE10/00020 (to JC), FIS09/00672 (to AX), SAF2010-22066-C02-02 (to AC), research grant from the Valencia Pneumology Foundation 2010 (to AD) and support from the CENIT programme, and research grants from Regional Government (Prometeo/2008/045, 'Generalitat Valenciana').

Competing interests None.

Patient consent Obtained.

Ethics approval This study was approved by the ethics committee of the University General Hospital of Valencia, Spain (CEIC28/2008).

Provenance and peer review Not commissioned; externally peer-reviewed.

REFERENCES

- 1 Lettieri CJ, Nathan SD, Barnett SD, et al. Prevalence and outcomes of pulmonary arterial hypertension in advanced idiopathic pulmonary fibrosis. *Chest* 2006;129:746–52.
- 2 Heath D, Gillund TD, Kay JM, et al. Pulmonary vascular disease in honeycomb lung. *J Pathol Bacteriol* 1968;95:423–30.

- 3 Blanco I, Ribas J, Xaubet A, et al. Effects of inhaled nitric oxide at rest and during exercise in idiopathic pulmonary fibrosis. *J Appl Physiol* 2011;110:638–45.
- 4 Hashimoto N, Phan SH, Imaizumi K, et al. Endothelial-mesenchymal transition in bleomycin-induced pulmonary fibrosis. *Am J Respir Cell Mol Biol* 2010;43:161–72.
- 5 Yeager ME, Frid MG, Stenmark KR. Progenitor cells in pulmonary vascular remodeling. *Pulm Circ* 2011;1:3–16.
- 6 Botney MD, Bahadori L, Gold LI. Vascular remodeling in primary pulmonary hypertension. Potential role for transforming growth factor-beta. *Am J Pathol* 1994;144:286–95.
- 7 Gaiad A, Yanagisawa M, Langleben D, et al. Expression of endothelin-1 in the lungs of patients with pulmonary hypertension. *N Engl J Med* 1993;328:1732–9.
- 8 Coggins MP, Bloch KD. Nitric oxide in the pulmonary vasculature. *Arterioscler Thromb Vasc Biol* 2007;27:1877–85.
- 9 Werner ER, Blau N, Thony B. Tetrahydrobiopterin: biochemistry and pathophysiology. *Biochem J* 2011;438:397–414.
- 10 Saleh D, Barnes PJ, Gaiad A. Increased production of the potent oxidant peroxynitrite in the lungs of patients with idiopathic pulmonary fibrosis. *Am J Respir Crit Care Med* 1997;155:1763–9.
- 11 Moens AL, Takimoto E, Tocchetti CG, et al. Reversal of cardiac hypertrophy and fibrosis from pressure overload by tetrahydrobiopterin: efficacy of recoupling nitric oxide synthase as a therapeutic strategy. *Circulation* 2008;117:2626–36.
- 12 Shimazu T, Otani H, Yoshioka K, et al. Sepiapterin enhances angiogenesis and functional recovery in mice after myocardial infarction. *Am J Physiol Heart Circ Physiol* 2011;301:H2061–72.
- 13 Cortijo J, Iranzo A, Milara X, et al. Roflumilast, a phosphodiesterase 4 inhibitor, alleviates bleomycin-induced lung injury. *Br J Pharmacol* 2009;156:534–44.
- 14 Ashcroft T, Simpson JM, Timbrell V. Simple method of estimating severity of pulmonary fibrosis on a numerical scale. *J Clin Pathol* 1988;41:467–70.
- 15 James AL, Hogg JC, Dunn LA, et al. The use of the internal perimeter to compare airway size and to calculate smooth muscle shortening. *Am Rev Respir Dis* 1988;138:136–9.
- 16 Haridas D, Chakraborty S, Ponnusamy MP, et al. Pathobiological implications of MUC16 expression in pancreatic cancer. *PLoS One* 2011;6:e26839.
- 17 Daniil ZD, Papageorgiou E, Koutsokera A, et al. Serum levels of oxidative stress as a marker of disease severity in idiopathic pulmonary fibrosis. *Pulm Pharmacol Ther* 2008;21:26–31.
- 18 Montes de Oca M, Torres SH, De Sanctis J, et al. Skeletal muscle inflammation and nitric oxide in patients with COPD. *Eur Respir J* 2005;26:390–7.
- 19 Gielis JF, Lin JY, Winkler K, et al. Pathogenetic role of eNOS uncoupling in cardiopulmonary disorders. *Free Radic Biol Med* 2011;50:765–76.
- 20 Nandi M, Miller A, Stidwill R, et al. Pulmonary hypertension in a GTP-cyclohydrolase 1-deficient mouse. *Circulation* 2005;111:2086–90.
- 21 Lee CK, Han JS, Won KJ, et al. Diminished expression of dihydropteridine reductase is a potent biomarker for hypertensive vessels. *Proteomics* 2009;9:4851–8.
- 22 Teng RJ, Du J, Xu H, et al. Sepiapterin improves angiogenesis of pulmonary artery endothelial cells with in utero pulmonary hypertension by recoupling endothelial nitric oxide synthase. *Am J Physiol Lung Cell Mol Physiol* 2011;301:L334–45.
- 23 Sawabe K, Yamamoto K, Harada Y, et al. Cellular uptake of sepiapterin and push-pull accumulation of tetrahydrobiopterin. *Mol Genet Metab* 2008;94:410–16.
- 24 Gao L, Pung YF, Zhang J, et al. Sepiapterin reductase regulation of endothelial tetrahydrobiopterin and nitric oxide bioavailability. *Am J Physiol Heart Circ Physiol* 2009;297:H331–9.
- 25 Hemnes AR, Zaiman A, Champion HC. PDE5A inhibition attenuates bleomycin-induced pulmonary fibrosis and pulmonary hypertension through inhibition of ROS generation and RhoA/Rho kinase activation. *Am J Physiol Lung Cell Mol Physiol* 2008;294:L24–33.
- 26 Jain R, Shaul PW, Borok Z, et al. Endothelin-1 induces alveolar epithelial-mesenchymal transition through endothelin type A receptor-mediated production of TGF-beta1. *Am J Respir Cell Mol Biol* 2007;37:38–47.
- 27 Willis BC, Borok Z. TGF-beta-induced EMT: mechanisms and implications for fibrotic lung disease. *Am J Physiol Lung Cell Mol Physiol* 2007;293:L525–34.
- 28 Arciniegas E, Frid MG, Douglas IS, et al. Perspectives on endothelial-to-mesenchymal transition: potential contribution to vascular remodeling in chronic pulmonary hypertension. *Am J Physiol Lung Cell Mol Physiol* 2007;293:L1–8.
- 29 Widyantoro B, Emoto N, Nakayama K, et al. Endothelial cell-derived endothelin-1 promotes cardiac fibrosis in diabetic hearts through stimulation of endothelial-to-mesenchymal transition. *Circulation* 2010;121:2407–18.
- 30 O'Riordan E, Mendeleev N, Patschan, et al. Chronic NOS inhibition actuates endothelial-mesenchymal transformation. *Am J Physiol Heart Circ Physiol* 2007;292:H285–94.
- 31 Xu H, Zaidi M, Struve J, et al. Abnormal fibrillin-1 expression and chronic oxidative stress mediate endothelial mesenchymal transition in a murine model of systemic sclerosis. *Am J Physiol Cell Physiol* 2011;300:C550–6.
- 32 Yoshimatsu Y, Watabe T. Roles of TGF-beta signals in endothelial-mesenchymal transition during cardiac fibrosis. *Int J Inflam* 2011;2011:724080.
- 33 Ramzy D, Rao V, Tumiaty LC, et al. Elevated endothelin-1 levels impair nitric oxide homeostasis through a PKC-dependent pathway. *Circulation* 2006;114(1 Suppl):1319–26.
- 34 Vyas-Read S, Shaul PW, Yuhanna IS, et al. Nitric oxide attenuates epithelial-mesenchymal transition in alveolar epithelial cells. *Am J Physiol Lung Cell Mol Physiol* 2007;293:L212–21.

Online data supplement

Role of tetrahydrobiopterin in pulmonary vascular remodeling associated with pulmonary fibrosis

Authors

Patricia Almudéver^{1*}, Javier Milara^{2,3,4,5*}, Alfredo De Diego⁶, Ana Serrano-Mollar^{5,7}, Antoni Xaubet^{5,8}, Francisco Perez-Vizcaino^{5,9}, Angel Cogolludo^{5,9} and Julio Cortijo¹,
2, 4, 5

¹Department of Pharmacology, Faculty of Medicine, University of Valencia, Spain

²Clinical research unit (UIC), University General Hospital Consortium, Valencia, Spain

³Department of Biotechnology, Universidad Politécnica de Valencia, Spain

⁴Research Foundation of General Hospital of Valencia, Spain

⁵CIBERES, Health Institute Carlos III, Valencia, Spain

⁶Servicio de Neumología, Hospital Universitario y Politécnico La Fe

⁷Dept de Patología Experimental, Instituto de Investigaciones Biomédicas de Barcelona, Consejo Superior de Investigaciones científicas

⁸Servicio de Neumología, Hospital Clínico, Instituto de Investigaciones Biomédicas Agustí Pi Suñer (IDIBAPS)

⁹Department of Pharmacology, School of Medicine, Universidad Complutense de Madrid

*Both authors contributed equally to this work

Corresponding Author: Javier Milara, PhD., Unidad de Investigación, Consorcio Hospital General Universitario, Avenida tres cruces s/n, E-46014 Valencia, Spain.
Phone: +34 620231549, Fax: +34961972145, E-mail: xmilara@hotmail.com

METHODS

Patients with Idiopathic Pulmonary Fibrosis

A total of 36 IPF patients (n=36 patients for plasma studies and n=17 for tissue studies) were included in the study. IPF was diagnosed according to the American Thoracic Society/European Respiratory Society (ATS/ERS) consensus criteria (1). Fibrotic lung samples were obtained at surgery for lung transplantation or by open lung biopsy for histological diagnosis of the disease. Matched plasma samples were obtained from peripheral venous blood of each patient. All pulmonary function tests were performed within 3 months before surgery. Inclusion criteria were defined as: 1) IPF patients free of symptoms of respiratory tract infection, and none received antibiotics perioperatively. 2) Patients with evident honeycombing and fibrosis. After selection based on diagnosis criteria, all lung tissue samples used for the study were checked histologically by using the following exclusion criteria: (1) presence of tumor. Clinical data is described in table 1. The protocol was approved by the local research and independent ethics committee of the University General Hospital of Valencia (CEIC28/2008). Informed written consent was obtained from each participant.

Control subjects

Age matched normal control lungs (n=21) were collected from patients undergoing thoracic surgery for removal of a primary lung tumour. Normal lung was obtained from a non-involved segment, remote from the solitary lesion. Plasma samples were obtained from age matched healthy subjects (n=30) without any medical disease. The biopsies taken from control donor lungs showed normal architecture with few intra-alveolar macrophages and edema.

Animal Model

Experimentation and handling were performed in accordance with the guidelines of the Committee of Animal Ethics and Well-being of the University of Valencia (Valencia, Spain). Rat studies used pathogen-free male wistar rats (Harlan Iberica[®], Barcelona, Spain) at 12 weeks of age which are reported to mount a robust early inflammatory response followed by pulmonary hypertension and fibrotic remodeling secondary to bleomycin (2). Rats were housed with free access to water and food under standard conditions: relative humidity 55 ± 10 %; temperature $22 \pm 3^{\circ}\text{C}$; 15 air cycles/per hour; 12/12 h Light/Dark cycle. Rats were anaesthetized with ketamine/medetomidine and then a single dose of bleomycin at 3.75 U/kg (dissolved in 200 μL of saline) was administered intratracheally via the endotracheal route (3). This dose of bleomycin reproducibly generated pulmonary fibrosis in previous experiments (4). Sham treated rats received the identical volume of intratracheal saline instead of bleomycin. This procedure fixed experimentation day **1** and was synchronously coupled with the initiation of sepiapterin treatment. Based on pharmacokinetic data (not shown) twice daily oral doses of sepiapterin (10 mg/Kg/b.i.d) were administered via an intra-esophageal cannula from day **1** to 21. Sepiapterin was prepared immediately prior to use. Sepiapterin was prepared with 0.4 % methocel/HCl (0.05 M) aqueous solution and ultrasounds in order to ensure complete dissolution. The control group received 0.4 % methocel/HCl (0.05 M) as vehicle. The account for experimental groups was estimated in a number of 10 rats (n=10): (i) saline serum + pharmaceutical vehicle; (ii) saline serum + sepiapterin (10 mg/Kg/b.i.d); (iii) bleomycin + pharmaceutical vehicle; (iv) bleomycin + sepiapterin (10 mg/Kg/b.i.d). With these doses of sepiapterin, no adverse effects were observed during the experiments. Results obtained for the group of saline serum + sepiapterin were identical to those of saline group. Therefore we did not

include because space restrictions in main manuscript. Rats were weighed each two days as an indicator of animal well-being and mortality was recorded during the 21 days of treatment. At the end of the treatment period (day 21), rats were sacrificed by a lethal injection of sodium pentobarbital followed by exsanguination. After opening the thoracic cavity, trachea, lungs and heart were removed *en bloc*. Lungs were weighed and then processed for histological, biochemical or molecular biology studies. The right ventricular (RV) wall of the heart was dissected free and weighed along with the left ventricle wall plus septum (LV + S), and the resulting weights are reported as RV/LV + S ratio to provide an index of right ventricular hypertrophy. Moments before sacrificing rats, femoral artery was cannulated and heparinized blood was collected for measurement of plasma BH₄, BH₂, nitrites and nitrotyrosine.

Hemodynamic Measurements

21 days after bleomycin/saline administration, 6 surviving rats of each experimental group were anesthetized with ketamine/medetomidine and measured for right ventricular systolic pressure (RVSP) by right heart catheterization. The right jugular vein was cannulated with a small silicone catheter (BPE-T50 Polyethylene tubing for 22ga swivels; Salomon Scientific, CA, USA) containing heparin saline solution (10 UI/ml of heparin in 0.9% saline), to reach the RV under the guidance of the pressure tracing. After 20 minutes of stabilization, RVSP was recorded using a miniature pressure transducer (TSD104A, BIOPAC Systems, Inc., CA, USA) digitized by a BIOPAC MP100 data acquisition system. The right carotid artery was cannulated in order to simultaneously measure systemic arterial pressure (SAP) with a transducer.

Histological, Immunohistochemical and Immunofluorescence Studies

Lung histology was conducted as previously reported (5). Tissue blocks (4 μm thickness) were stained with haematoxylin-eosin for assessment of the fibrotic injury and pulmonary artery remodeling, and with Masson's trichrome (Sigma-Aldrich, Madrid, Spain) to detect collagen deposition. Severity of lung fibrosis was scored on a scale from 0 (normal lung) to 8 (total fibrotic obliteration of fields) according to Ashcroft (6). To determine the extent of pulmonary vascular remodeling, the degree of muscularization of intraacinar pulmonary vessels was determined. Lung sections (4 μm thickness) were stained with haematoxylin-eosin, and mouse monoclonal anti- α -smooth muscle actin (1:200 v/v) and analysed using a morphometric system (Olympus BH2 Research Microscope, Olympus America Inc, Center Valley, PA, USA) with the software package Image ProPlus 5.0 (MediaCybernetics, Silver Spring, MD, USA). In each animal, 25–40 intraacinar arteries with an external diameter between 20 and 50 μm were analysed. The measurements made include internal area (IA), the external perimeter (EP) and the external area (EA), defined by the outer edge of the smooth muscle layer. The absolute wall area (WA) was calculated with the following formula: $WA=EA-IA$ (7). All measurements were made by the same observer. The pulmonary artery wall thickness was calculated by dividing the WA by the EP as previously outlined (7).

For immunohistochemical analysis of rat and human lungs, tissue was fixed and embedded in paraffin, cut into sections (4-6 μm) and incubated with mouse anti-rat/human α -SMA (cat. n^o: A5228; Sigma), goat anti-rat/human SPR (cat. n^o: sc-169414; Santa Cruz Biotechnology, inc), mouse anti- rat/human GCH-1 (cat. n^o: sc-271482; Santa Cruz Biotechnology), rabbit anti-rat/human eNOS (cat. n^o: RB-1711-PO; ThermoScientific) and rabbit anti- rat/human iNOS (cat. n^o: RB-1605 NeoMarkers, Fremont, CA) for 24 h at 4°C. A secondary anti-rabbit goat or anti-mouse antibody

(1:100; Vector Laboratories, Burlingame, CA) with avidin-biotin complex/horseradish peroxidase was used for immunohistochemistry. The non-immune IgG isotype control was used as negative control and gave negative for all samples.

All stained slides were scored by a pathologist under a Nikon Eclipse TE200 (Tokio, Japan) light microscope and representative photographs taken (10 slices per patient) as previously outlined (8). Staining intensity for different antibodies was scored on a scale of 0–3 (0-negative, 1-weak, 2-moderate, 3-strong immunoreactivity). The percentage of cells positive for different antibodies within pulmonary artery was scored on a scale of 1–4 as follows: 1: 0–25% cells positive; 2: 26–50% positive; 3: 51–75% positive; and 4: 76–100% positive. The score of the staining intensity and the percentage of immunoreactive cells were then multiplied to obtain a composite score ranging from 0 to 12.

For immunofluorescence, human pulmonary artery endothelial cells (HPAECs), human pulmonary airway tissue, or rat pulmonary airway tissue were washed three times with PBS and fixed (4% paraformaldehyde, 24 h, at room temperature). After another three washes with PBS, lung tissue was included in O.C.T™ compound (tissue-Tek, USA) and fridge at -80°C to be sectioned in 14µm with a cryotome (leica, Spain). The slices obtained were permeabilized (20 mM HEPES pH 7.6, 300 mM sucrose, 50 mM NaCl, 3 mM MgCl₂, 0.5% Triton X-100), blocked (10% goat serum in PBS) and incubated with the primary antibody mouse anti-human CD31 monoclonal antibody (IS610; dako, Madrid Spain), rabbit anti-human VE-cadherin polyclonal antibody (VI514; sigma, Madrid Spain), mouse anti-human α -SMA monoclonal antibody (A5228; sigma, Madrid Spain) or rabbit anti-human collagen type I polyclonal antibody (234167; Calbiochem Darmstadt, Germany) overnight at 4°C, followed by secondary antibody anti-mouse rhodamine (1:100, Molecular Probes) or anti-rabbit-FITC (1:100 Molecular

probes) and DAPI to mark nuclei. Slices were mounted using fluorescent mounting medium (Dako, Spain). Cells were visualized by fluorescence microscopy ($\times 200$; Nikon eclipse TE200 inverted microscope, Tokyo, Japan). IgG isotype controls gave always negative immunofluorescence signal.

Determination of BH₄/BH₂, Nitrites and Nitrotyrosine

To measure BH₄ and BH₂ plasma and pulmonary artery tissue levels, venous blood or isolated and homogenized pulmonary artery tissue were collected in EDTA tubes containing either 0.1% (w/v) dithioerythritol (DTE) as antioxidant. After exactly 3h at room temperature, it was centrifuged at 2000g, for 10 min, and plasma was stored at -80 °C as previously outlined (9). Total biopterin equals the combined sum of 7, 8-dihydrobiopterin (BH₂), BH₄ and fully oxidized biopterin. Differential oxidation mediated by iodine permits the measurement of BH₄ concentration. Under acidic conditions BH₄ and BH₂ are oxidized to biopterin, while under basic conditions only BH₂ is oxidized to biopterin, and BH₄ undergoes side-chain cleavage to form pterin. The difference in biopterin content between the two oxidations represents the actual BH₄ levels (10). In brief, the acidic oxidation was realized as follows: 90 μ l of plasma and 10 μ l of the internal standard (rhamnopterin 400 nM) were acidified by the addition of 20 μ l HCl (1M) and 50 μ l of I₂/IK solution (1% (w/v) iodine in 2 % (w/v) potassium iodide). Samples were mixed and incubated for 1 h in the dark at room temperature. The reaction was stopped adding 10 μ l of 5 % (w/v) ascorbic acid and 20 μ l of water. The basic condition was identical to the preparation of the acidic condition with the exception that HCl was substituted by the addition of 20 μ l NaOH (1M). Samples were added, mixed and incubated for 1 h in obscurity at room temperature followed by the addition of 10 μ l of 5 % (w/v) ascorbic acid and 20 μ l HCl (2M).

The HPLC system consisted of a Shimadzu LC-10ADvp isocratic pump, Shimadzu SIL-10ADvp auto-injector, Shimadzu RF10Avp fluorescence detector and Shimadzu SCL-10Avp controller. HPLC system control and data processing were performed by Shimadzu LCM Solutions software (Shimadzu, Tokyo, JP). The analytical method was validated in our laboratory in accordance to FDA Guidance for Industry (11). The separation was performed as described by Fiege et al (12). The stationary phase included precolumn and column Sherisorb ODS1 5 μ m (4.6 x 250 mm; Waters® Barcelona, Spain), and a mobile phase consisting in 1.5 mmol/L potassium hydrogen phosphate at pH 4.6 with 10% methanol, at a flow rate of 1 mL/min at room temperature. The fluorescence detector was set at 350nm (excitation) and 450nm (emission). Prior to inject into the HPLC system, samples were filtered through a 10000 MW microfilter (Multiscreen, Millipore®) at 3000g for 1h at 10°C for physical desproteinisation. Quantification of BH4 and BH2 was made by interpolation to a standard curve of biopterin (1, 5, 10, 25, 50, 75 y 100 ng/ml).

NO was quantitatively determined in plasma and in HPAEC supernatants using a commercially available NO assay kit (Calbiochem-Novabiochem, San Diego, CA) based on the enzymatic conversion of nitrate to nitrite (NOx) by nitrate reductase according to the manufacturer's instructions. Nitrotyrosine was determined in plasma and in HPAEC supernatants using a commercially available ELISA (Hycult biotech, HK501)

Human Pulmonary Artery Endothelial cell isolation and *in vitro* experimental conditions

Cellular experiments were performed in HPAECs isolated from pulmonary arteries of normal lungs. Segments of pulmonary artery (2-3 mm internal diameter) were dissected

free from parenchyma lung tissue, cut longitudinally, and digested with 1% collagenase (Gibco, UK) in RPMI-1640 culture medium for 30 min at 37°C. The digestion was neutralized by adding RPMI 1640 supplemented with 20% foetal calf serum (FCS), and the homogenate was separated by centrifugation at 1100 rpm. The pellet was resuspended, and cells were cultured in EGM-2 endothelial culture medium supplemented with Single Quotes (Clonetics, UK), 10% FCS, 1% fungizone, and 2% streptomycin/penicillin. The selection of HPAECs was performed as described previously (13, 14), modified to include the use of a commercially available Dynabeads CD31 endothelial cell kit (DynaL Biotech, Germany). Briefly, cells were trypsinized (0.25% trypsin), and the cell mixture was incubated with CD-31-coated Dynabeads for 30 min at 4°C with end-over-end rotation. After incubation, the HPAECs were collected using a magnetic particle concentrator (MCP-1; Dynal) and washed four times with cold phosphate-buffered saline (PBS)/bovine serum albumin (BSA). Clusters of purified HPAECs retained on the CD-31-coated Dynabeads were separately resuspended in EGM-2 full growth medium supplemented with 10% FCS, 1% fungizone, and 2% streptomycin/penicillin. The cells not retained on the CD-31-coated Dynabeads were discarded.

For *in vitro* studies, HPAECs were stimulated with TGF- β 1 (5ng/ml; Sigma) or ET-1 (100nM; Sigma) for the indicated times, replacing culture medium and stimulus every 24 h. The antioxidant N-acetyl-L-cysteine (1mM; NAC; Sigma), SIS3 (described as Smad3 inhibitor, 10 μ M; Sigma) and sepiapterin (1 μ M-100 μ M; Schircks Laboratories, Buechstrasse, CH) were added 30 min before stimulus and remained together with the stimulus. Monoclonal anti-human TGF- β 1 mAb (4 μ g/mL; anti-TGF- β 1; R&D Systems, Madrid, Spain) was added 30 min before stimulus to block the active form of TGF- β 1 present in the culture supernatant as previously outlined (15).

Real Time RT-PCR

Total RNA was isolated from rat lung tissue, primary HPAECs and pulmonary arteries from IPF patients by using TriPure[®] Isolation Reagent (Roche, Indianapolis, USA). The integrity of the extracted RNA was confirmed with Bioanalyzer (Agilent, Palo Alto, CA, USA). The reverse transcription was performed in 300 ng of total RNA with TaqMan reverse transcription reagents kit (Applied Biosystems, Perkin-Elmer Corporation, CA, USA). cDNA was amplified with specific primers and probes predesigned by Applied Biosystems for, collagen type I (col type I; cat. n°: Rn01463848_m1), connective tissue growth factor (CTGF; cat. n°: Rn00583793_m1), transforming growth factor beta 1 (TGF- β 1; cat. n°: Rn00572010_m1), endothelin 1 (ET-1; cat. n°: Rn00561129_m1) iNOS (cat. n°: Hs01075529_m1), eNOS (cat. n°: Hs01574659_m1), GCH-1 (cat. n°: Hs00609198_m1), and SPR (cat. n°: Hs00268403_m1) and GAPDH (pre-designed by Applied Biosystems, cat. n°: 4308313/rat and 4352339/human) as a housekeeping in a 7900HT Fast Real-Time PCR System (Applied Biosystem) using Universal Master Mix (Applied Biosystems). Relative quantification of these different transcripts was determined with the $2^{-\Delta\Delta C_t}$ method using GAPDH as endogenous control (Applied Biosystems; 4352339E) and normalized to control group.

To determine the relative expression of the α -SMA, sm22- α , snail, slug, CD31, VE-cadherin and vegfr SYBR Green real-time PCR was used. Primer sequences are defined in table 1. The percentage primer efficiency and correlation coefficients of the SYBR Green primers was calculated and accepted for efficiencies $100 \pm 10\%$. The amplification specificity for each RT-PCR analysis was confirmed by melting curve analysis. 4 μ l of cDNA was added to 19 μ l of reaction mixture containing 7 μ l H₂O, 10 μ l QuantiTect[®] SYBR[®] Green PCR Master Mix (Qiagen, UK) and 1 μ l each of forward

and reverse primers (10 μ M) (Table 1). Relative quantification of transcript levels (compared to control groups) was determined by evaluating the expression as $2^{-\Delta\Delta CT}$ as described above.

Table 1. Primers for SYBR Green real-time quantitative reverse transcriptase polymerase chain reaction.

	Forward	Reverse
Gapdh	CACCAACTGCTTAGCACCCC	TCTTCTGGGTGGCAGTGATG
Slug	TGCGATGCCCAGTCTAGAAA	TGCAGTGAGGGCAAGAAAAA
Snail	CCCAGTGCCTCGACCACTAT	CCAGATGAGCATTGGCAGC
α -SMA	TTTCCGCTGCCCAGAGAC	GTCAATATCACACTTCATGATGCTGT
sm22- α	CCGGTTAGGCCAAGGCTC	GCGGCTCATGCCATAGGA
CD31	AAAGTCGGACAGTGGGACGT	GGCTGGGAGAGCATTTCACA
VE-cadherin	GATGCAGACGACCCCACTGT	CCACGATCTCATACTGGCC
VegfR	TCAGGCAGCTCACAGTCCTAGA	ACTTGTCGTCTGATTCTCCAGGTT

Western blot

Western blot analysis was used to detect changes of TGF- β 1, ET-1 and p-Smad3 in lung tissue and HPAECs. Lung tissue from rats and HPAECs were homogenized and lysed on ice with a lysis buffer consisting of 20mM Tris, 1 mM ethylenediaminetetraacetic acid (EDTA), 150mM NaCl, 0.1% Triton X-100, 1 mM dithiothreitol and 1 μ g/ml pepstatin A supplemented by a complete protease inhibitor cocktail. The Bio-Rad assay (Bio-Rad Laboratories Ltd., Herts, UK) was used to quantify the level of protein in each sample to ensure equal protein loading. Sodium dodecyl sulphate polyacrylamide gel electrophoresis was used to separate the proteins according to their molecular weight. Briefly, 10 μ g proteins (denatured) along with a molecular weight protein marker, Bio-Rad Kaleidoscope marker (Bio-Rad Laboratories), were loaded onto an acrylamide gel

consisting of a 5% acrylamide stacking gel stacked on top of a 10% acrylamide resolving gel and run through the gel by application of 100 V for 1 h. Proteins were transferred from the gel to a polyvinylidene difluoride membrane using a wet blotting method. The membrane was blocked with 5% Marvel in PBS containing 0.1% Tween20 (PBS-T) and then probed with a rabbit anti-rat TGF- β 1 (cat. n $^{\circ}$: 3709S; Cell Signaling Technology Inc., Barcelona, ES), mouse anti-rat ET-1 (cat. n $^{\circ}$: MA3-005; Thermo Scientific, IL, US) and rabbit anti-human phospho-Smad3 (cat. n $^{\circ}$: PS1023; Calbiochem), and normalised to total mouse anti-rat β -actin antibody (cat n $^{\circ}$: A1978; Sigma) or total rabbit anti-human Smad3 (cat n $^{\circ}$: 566414; Calbiochem) as house-keeping reference, followed by the corresponding peroxidase-conjugated secondary (1:10,000) antibody. The enhanced chemiluminescence method of protein detection using ECL-plus (GE Healthcare, Amersham Biosciences, UK) was used to detect labelled proteins. Quantification of protein expression was performed by densitometry relative to total Smad3 expression using the software GeneSnap version 6.08.

DCF Fluorescence Measurement of Reactive Oxygen Species

2', 7'-dichlorodihydrofluorescein diacetate (H₂DCF-DA, Molecular Probes, UK) is a cell-permeable compound that following intracellular ester hydrolysis is oxidized to fluorescent 2', 7'-dichlorofluorescein (DCF) by O₂⁻ and H₂O₂, and can therefore be used to monitor intracellular generation of ROS (16). To quantify ROS levels, HPAECs were seeded to black walled, clear bottom 96 well plates, washed twice with PBS and incubated for 30 min with 50 μ M H₂DCF-DA diluted in Opti-MEM in presence or absence of sepiapterin (1 μ M-100 μ M). Then, cells were again washed twice with PBS to remove remaining H₂DCF-DA and stimulated with TGF- β 1 (5ng/ml) or ET-1 (100nM) for 30 min in presence or absence of sepiapterin. Five randomly selected fields per

condition were measured for fluorescent intensity using an epifluorescence microscope (Nikon Eclipse TE 200, Tokio, Japan) with filter set for FITC. Subsequent image capture and analysis was performed using Metafluor[®] 5.0 software (Analytical Technologies, US). Results were expressed as DCF fluorescence in relative fluorescence units (RFU).

Statistics

Statistical analysis of results was carried out by parametric (animal and cellular studies) or non-parametric (human studies) analysis as appropriate. $P < 0.05$ was considered statistically significant. Non-parametric tests were used to compare results from human samples of control patients and IPF patients. In this case, data were displayed as medians, interquartile range and minimum and maximum values. When the comparisons concerned only 2 groups, between-group differences were analyzed by the Mann Whitney test. Results from animal and cellular *in vitro* mechanistic cell experiments (Figures 1-6 in main manuscript) were expressed as mean \pm SE of n experiments since normal distribution for each data set was confirmed by histogram analyses and Kolmogorov–Smirnov test. In this case, statistical analysis was carried out by parametric analysis. Two-group comparisons were analysed using the two-tailed Student's paired t-test for dependent samples, or unpaired t-test for independent samples. Multiple comparisons were analysed by one-way or two-way analysis of variance followed by Bonferroni post hoc test. Statistical analysis was done on raw data considered as the gene expression corrected by the housekeeping GAPDH, protein expression corrected by the internal standards Smad3 as appropriate. Analysis of levels of BH4, BH4/BH2, nitrotyrosine, nitrites and DCF fluorescence were performed on raw data.

Online References

1. American thoracic society. Idiopathic pulmonary fibrosis: Diagnosis and treatment. International consensus statement. American thoracic society (ats), and the european respiratory society (ers). *Am J Respir Crit Care Med* 2000;161:646-664.
2. Hemnes AR, Zaiman A, Champion HC. Pde5a inhibition attenuates bleomycin-induced pulmonary fibrosis and pulmonary hypertension through inhibition of ros generation and rhoa/rho kinase activation. *Am J Physiol Lung Cell Mol Physiol* 2008;294:L24-33.
3. Bivas-Benita M, Zwier R, Junginger HE, Borchard G. Non-invasive pulmonary aerosol delivery in mice by the endotracheal route. *Eur J Pharm Biopharm* 2005;61:214-218.
4. Mata M, Ruiz A, Cerda M, Martinez-Losa M, Cortijo J, Santangelo F, Serrano-Mollar A, Llombart-Bosch A, Morcillo EJ. Oral n-acetylcysteine reduces bleomycin-induced lung damage and mucin muc5ac expression in rats. *Eur Respir J* 2003;22:900-905.
5. Cortijo J, Iranzo A, Milara X, Mata M, Cerda-Nicolas M, Ruiz-Sauri A, Tenor H, Hatzelmann A, Morcillo EJ. Roflumilast, a phosphodiesterase 4 inhibitor, alleviates bleomycin-induced lung injury. *Br J Pharmacol* 2009;156:534-544.
6. Ashcroft T, Simpson JM, Timbrell V. Simple method of estimating severity of pulmonary fibrosis on a numerical scale. *J Clin Pathol* 1988;41:467-470.
7. James AL, Hogg JC, Dunn LA, Pare PD. The use of the internal perimeter to compare airway size and to calculate smooth muscle shortening. *Am Rev Respir Dis* 1988;138:136-139.

8. Haridas D, Chakraborty S, Ponnusamy MP, Lakshmanan I, Rachagani S, Cruz E, Kumar S, Das S, Lele SM, Anderson JM, Wittel UA, Hollingsworth MA, Batra SK. Pathobiological implications of muc16 expression in pancreatic cancer. *PLoS One* 2011;6:e26839.
9. Fekkes D, Voskuilen-Kooijman A. Quantitation of total biopterin and tetrahydrobiopterin in plasma. *Clin Biochem* 2007;40:411-413.
10. Fukushima T, Nixon JC. Analysis of reduced forms of biopterin in biological tissues and fluids. *Anal Biochem* 1980;102:176-188.
11. Guidance for industry. Bioanalytical method validation.: Food and Drug Administration. U. S 2001.
12. Fiege B, Ballhausen D, Kierat L, Leimbacher W, Goriounov D, Schircks B, Thony B, Blau N. Plasma tetrahydrobiopterin and its pharmacokinetic following oral administration. *Mol Genet Metab* 2004;81:45-51.
13. Hewett PW, Murray JC. Immunomagnetic purification of human microvessel endothelial cells using dynabeads coated with monoclonal antibodies to pecam-1. *Eur J Cell Biol* 1993;62:451-454.
14. Ortiz JL, Milara J, Juan G, Montesinos JL, Mata M, Ramon M, Morcillo E, Cortijo J. Direct effect of cigarette smoke on human pulmonary artery tension. *Pulm Pharmacol Ther* 2009.
15. Milara J, Serrano A, Peiro T, Gavalda A, Miralpeix M, Morcillo EJ, Cortijo J. Aclidinium inhibits human lung fibroblast to myofibroblast transition. *Thorax* 2011.
16. Trayner ID, Rayner AP, Freeman GE, Farzaneh F. Quantitative multiwell myeloid differentiation assay using dichlorodihydrofluorescein diacetate (h2dcf-da) or dihydrorhodamine 123 (h2r123). *J Immunol Methods* 1995;186:275-284.